Synthesis and study of decay properties of the doubly magic nucleus ^{270}Hs in the ^{226}Ra + ^{48}Ca reaction

Yu. Ts. Oganessian,[1,*] V. K. Utyonkov,[1] F. Sh. Abdullin,[1] S. N. Dmitriev,[1] R. Graeger,[2] R. A. Henderson,[3] M. G. Itkis,[1] Yu. V. Lobanov,[1] A. N. Mezentsev,[1] K. J. Moody,[3] S. L. Nelson,[3] A. N. Polyakov,[1] M. A. Ryabinin,[4] R. N. Sagaidak,[1] D. A. Shaughnessy,[3] I. V. Shirokovsky,[1] M. A. Stoyer,[3] N. J. Stoyer,[3] V. G. Subbotin,[1] K. Subotic,[1] A. M. Sukhov,[1] Yu. S. Tsyganov,[1] A. Türler,[2] A. A. Voinov,[1] G. K. Vostokin,[1] P. A. Wilk,[3] and A. Yakushev[2]

[1]*Joint Institute for Nuclear Research, RU-141980 Dubna, Russian Federation*

[2]*Technische Universität München, D-85748 Garching, Germany*

[3]*Lawrence Livermore National Laboratory, Livermore, California 94551, USA*

[4]*Research Institute of Atomic Reactors, RU-433510 Dimitrovgrad, Russian Federation*

(Received 28 September 2012; published 5 March 2013)

Production and decay of the isotopes of Hs were studied in the ^{226}Ra + ^{48}Ca reaction at beam energies $E_{\rm lab} = 229$, 234, and 241 MeV. At the $E_{\rm lab} = 234$ MeV energy, the maximum of the $4n$-evaporation channel of the reaction, six identical α-SF decay chains of the nucleus ^{270}Hs were detected corresponding to a cross section of $\sigma_{4n} = 16^{+13}_{-7}$ pb. At the other ^{48}Ca energies, no Hs isotopes were observed. Nuclei of ^{270}Hs undergo α decay with a $Q_\alpha = 9.15 \pm 0.08$ MeV and the half-life of the daughter spontaneous fission (SF) isotope ^{266}Sg is $0.28^{+0.19}_{-0.08}$ s, in good agreement with the data previously observed in the ^{248}Cm(^{26}Mg,$4n$)^{270}Hs reaction. The partial α-decay half-life of ^{270}Hs was measured for the first time: $T_\alpha = 7.6^{+4.9}_{-2.2}$ s. For the spontaneous fission, we determined a lower limit $T_{\rm SF} \geqslant 10$ s. Decay properties of ^{270}Hs corroborate theoretical predictions of its relatively high stability caused by the effect of the deformed shells at $Z = 108$ and $N = 162$.

DOI: 10.1103/PhysRevC.87.034605 PACS number(s): 27.90.+b, 23.60.+e, 25.70.Gh

I. INTRODUCTION

According to the predictions of microscopic theory, the existence of the heaviest elements is fully controlled by the closed deformed shells at $Z = 108$, $N = 162$ and spherical shells in heavier nuclei at $Z = 114$ (or possibly 120–126) and $N = 184$. In the studies carried out in recent years, a group of nuclides with $Z = 104$–118 and $N = 161$–177 was synthesized [1–12]. By and large, the experimental data on the decay properties of more than 50 new nuclei agree well with the theoretical predictions. This provides direct evidence of the manifestation of the new closed shells in the region of the heaviest nuclei that considerably expand the limits of the existence of chemical elements.

In this respect, of great interest to study directly are the doubly magic nuclei: deformed ^{270}Hs and spherical ^{298}114 (or ^{304}120, ^{310}126 in other models). In their decay, the stabilizing shell effect should be maximum. While synthesis of the neutron-rich spherical nuclei with $N \approx 184$ is a difficult task, the nuclide ^{270}Hs can be produced with several reactions.

The doubly magic nucleus ^{270}Hs was studied for the first time in the reaction ^{248}Cm(^{26}Mg,$4n$)^{270}Hs [2,3]. At the excitation energy of $E^* = 40$–49 MeV, near the maximum of the cross section of the $4n$-evaporation channel, six α-SF chains were detected that were assigned to the decay of ^{270}Hs produced with the cross section of $\sigma_{4n} \approx 3$ pb. The nuclide ^{270}Hs was found to emit α particles with $E_\alpha = 8.88 \pm 0.05$ MeV and give birth to the daughter ^{266}Sg that undergoes spontaneous fission (SF) with a half-life of $T_{1/2} = 0.36^{+0.25}_{-0.10}$ s [3]. In a later experiment, only a single decay of ^{270}Hs ($E_\alpha = 9.02^{+0.05}_{-0.10}$ MeV) that was followed in 23 ms by SF of ^{266}Sg was registered in the ^{238}U + ^{36}S reaction [13]. In these experiments, the signals from the implantation of the recoil nuclei in the detector were not registered; as a result, the half-life of the evaporation residue is not measured. For the same reason, the half-life of the SF of the mother nucleus is also not determined. Another possible synthesis reaction, ^{244}Pu(^{30}Si,$4n$)^{270}Hs, has not been studied yet. Finally, in the symmetric cold fusion ^{136}Xe(^{136}Xe,$2n$)^{270}Hs reaction, only an upper limit of the cross section $\sigma_{1n-3n} \leqslant 4$ pb [14] was determined.

However, the ^{226}Ra + ^{48}Ca reaction looks the most promising for synthesizing ^{270}Hs. Due to the doubly magic ^{48}Ca projectile, the excitation energy of the compound nucleus ^{274}Hs with beam energies at the Coulomb barrier decreases down to 32 MeV [15] and the expected cross section of the $4n$-evaporation channel could increase up to 30 pb [16,17]. Studies of the decay properties of the isotopes of Hs could be continued with better statistics in this reaction.

Measuring the cross sections of the production of evaporation residues in the ^{226}Ra + ^{48}Ca reaction is of individual interest within systematic studies of formation and survival of heavy compound nuclei in the reactions with ^{48}Ca. Production of Hs isotopes is an intermediate case between the well-studied cold fusion reactions of spherical colliding nuclei $^{206-208}$Pb(^{48}Ca,xn)$^{(254-256)-x}$No (see, e.g., Refs. [18,19] and references therein) and reactions of fusion of the deformed target nuclei of ^{238}U, ^{237}Np, ^{242,244}Pu, ^{243}Am, ^{245,248}Cm, ^{249}Bk, and ^{249}Cf with ^{48}Ca that we have used for synthesizing the superheavy elements (SHE) [1,10–12].

Despite the difficulties arising from using a highly α-radioactive target of ^{226}Ra (21–33 mCi, including daughter nuclei), in 2008 and 2009, we performed experiments aimed

*oganessian@jinr.ru

at the production of Hs isotopes with the ^{226}Ra + ^{48}Ca reaction.

II. EXPERIMENTAL TECHNIQUE

The α-radioactive isotope ^{226}Ra ($T_{1/2} = 1600$ y) target was deposited as an oxide RaO onto 1.5-μm-thick Ti foils. The total area of the rotating target was 36 cm^2. In the experiment, we used targets with Ra thicknesses of 0.12 and 0.18 mg/cm^2 (see Table I). In the course of the irradiation with the ^{48}Ca beam, the target thickness was checked periodically by measuring the ^{226}Ra α-particle counting rate.

The ^{48}Ca beam was obtained at the U400 cyclotron of the FLNR, JINR. The typical beam intensity at the target position was 0.7–1.1 pμA. The beam energy was measured by employing a time-of-flight system with a systematic uncertainty of 1 MeV.

The Dubna gas-filled recoil separator (DGFRS) [20,21] was used to separate evaporation residues (ER) from ^{48}Ca ions, scattered particles, and transfer-reaction products and deliver them to the focal-plane detectors. The transmission efficiency for Hs isotopes was estimated to be approximately 40%. At the focal plane of the separator, ERs passed through a time-of-flight system and were implanted in a 4-cm× 12-cm semiconductor detector array with 12 vertical position-sensitive strips surrounded by 8 4-cm×4-cm side detectors without position sensitivity, forming a box open to the front (beam) side. The position-averaged detection efficiency for full-energy α particles emitted in the decays of the implanted nuclei was 87%.

The detectors were tested by registering the recoil nuclei, α particles, and SF fragments from the decay of the known isotopes of Th, No, and their descendants produced in the reactions $^{\text{nat}}$Yb(^{48}Ca,xn) and ^{206}Pb(^{48}Ca,2n), respectively. The full width at half maximum (FWHM) energy resolutions for α particles absorbed in the focal-plane detector were 50–110 keV (depending on strip) and 130–310 keV for α particles that escaped this detector with a low-energy release and were registered by a side detector. Fission fragments from the decay of ^{252}No implants were used for the total-kinetic-energy calibration. The measured fragment energies should be corrected for the pulse-height defect of the detectors and for energy losses of escaping fragments in the detectors' entrance windows, dead layers, and the pentane gas filling the detection system. The mean sum energy loss of fission fragments of ^{252}No registered by both the focal-plane and side detectors was 20–25 MeV; the detection efficiency of such double fission events was about 40%. The FWHM position resolutions of correlated ER-α and ER-SF signals were 1.1–1.9 and 0.6–1.6 mm, respectively. For α particles detected by both the focal-plane and side detectors, the ER-α position resolution depends on the energy deposited in the focal-plane detector and was on average 2.0–3.5 and 3.4–5.8 mm for energies larger and lower than 3 MeV, respectively.

TABLE I. ^{226}Ra target thicknesses, average laboratory-frame beam energies in the middle of the target used in this work, corresponding average excitation energies, total accumulated beam doses, and number of events assigned to decays of Hs nuclei.

Target thickness (mg/cm^2)	E_{lab} (MeV)	E^* (MeV)	Beam dose ($\times 10^{18}$)	Number of events
0.12	229	34.7–38.5	2.9	0
0.18	229	34.7–38.7	3.3	0
0.12	234	38.2–42.8	3.0	4
0.18	235	39.0–43.2	1.1	2
0.18	241	44.6–48.7	2.3	0

The experimental conditions are summarized in Table I. Excitation energies of the compound nucleus at given projectile energies are calculated using the published masses of Refs. [22,23], taking into account the thickness of the targets and the energy spread of the incident cyclotron beam. The energy loss of the beam was calculated using the published data tables of Refs. [24,25].

For detection of the daughter nuclides in the absence of beam-associated background, the beam was switched off after a recoil signal was detected with implantation energy $E_{\text{ER}} =$ 9–15 MeV (expected for evaporation residues) followed by an α-like signal with an energy of $9.0 \leqslant E_\alpha \leqslant 9.38$ MeV (expected for decays of ^{269}Hs and ^{271}Hs) in the same strip, within a 2.2-mm-wide position window and a time interval of $\Delta t \leqslant 8$ s. Because of the short half-life of the SF daughter ^{266}Sg ($T_{1/2} = 0.36$ s) in α-SF decay of ^{270}Hs nucleus [3], and the low counting rate of SF-like events (see below), real decays of ^{270}Hs can be easily found in the data, so part of the experiment at $E_{\text{lab}} = 234$ MeV with the 0.12-mg/cm^2 target was conducted without switching off the beam. All other experiments shown in Table I were performed with 3-min beam-off intervals for detection of more long-lived decay products of even-odd Hs isotopes. In the experiment at high ^{48}Ca energy, the duration of beam-off time interval was 1 min, but if a particle with $E_\alpha = 8.5$–9.1 MeV was registered in any position of the same strip, the beam-off interval was automatically extended to 3 min.

III. EXPERIMENTAL RESULTS

Experiments were carried out at three beam energies (see Table I). The $E_{\text{lab}} = 234$ MeV energy corresponds to the maximum of the 4n-evaporation channel leading to ^{270}Hs [17]. At two other energies of 229 and 241 MeV, the yield of ^{270}Hs should be lower; they are more optimal for the production of neighboring isotopes ^{271}Hs and ^{269}Hs in 3n and 5n channels, respectively.

In two runs performed at the energy of 234 MeV with two targets of different thickness, six correlated decay chains of the type ER-α-SF were observed (see Table I). The measured parameters of the observed events are shown in Fig. 1. Energies of events, their positions, and time intervals are presented. The energies of events detected by both the focal-plane and the side detectors are shown in brackets. The energy resolution ΔE is given for each α particle. Most of the first experiment was performed without beam interruptions. In one chain observed in the second run in strip 4, the ER-α pair did

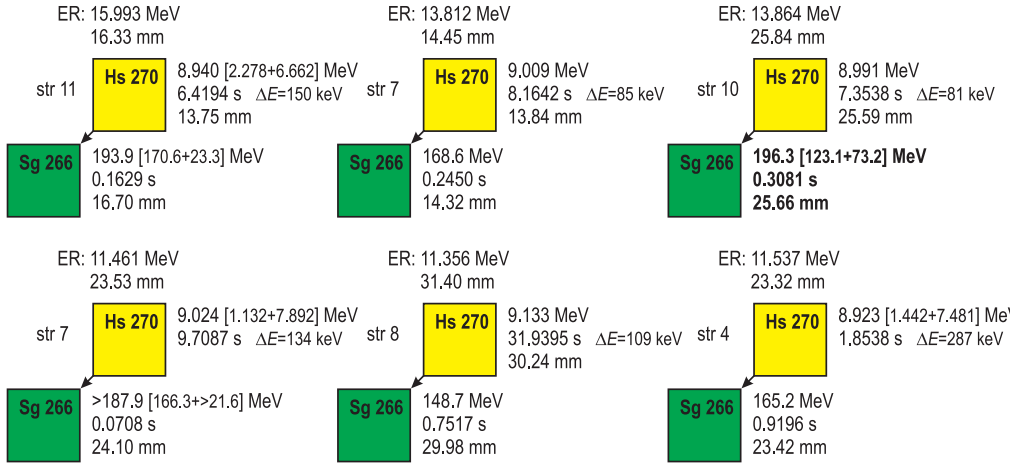

FIG. 1. (Color) Decay chains observed in the ^{226}Ra + ^{48}Ca reaction. Strip numbers (str), energies, energy resolution (ΔE), times between events, and positions of events are shown.

not switch the beam off because of the low-energy α particle deposited in the focal-plane detector and its position signal was below the electronic threshold. In another decay, the fission event was detected when the beam was off (event marked in boldface). In one case (left bottom, strip 7), the fission fragments were registered by both detectors. The energy of the fragment in the side detector exceeded the α-scale interval but was not detected in the high-energy scale. Therefore, the energy of fragment registered by the side detector was larger than 21.6 MeV and total measured energy was larger than 187.9 MeV.

In the analysis of the data, we found seven sequences of the type ER ($E = 7.5$–16.5 MeV)-α ($E = 8.7$–9.5 MeV, $\Delta t \leqslant 60$ s)-SF ($\Delta t \leqslant 400$ s) within position windows corresponding to two FWHM position resolutions (confidence level 0.98). In one case, the α-SF time interval was 285 s. The six other decay chains are shown in Fig. 1. All these SF events were registered within 1 s after preceding α decays. Thus, the total number of random ER-α-SF ($\Delta t \leqslant 1.4$ s $\approx 5T_{\rm SF}$ of the daughter nucleus) decay chains is less than 0.025 [26].

The distribution (number of events versus time interval in double logarithmic scale) for all ER-like events preceding the α-SF chains shown in Fig. 1 and registered within two ER-α or ER-SF position resolutions is shown in Fig. 2. For all 6 decay chains, 54 ER-like events were found within a 4000-s time interval which indicates that the total number of random ER-like events detected during 5 half-lives of the parent nucleus (38 s) is about 0.5 [26].

The α-particle energy and half-life of the parent nucleus are $E_\alpha = 9.02 \pm 0.08$ MeV, $T_{1/2} = 7.6^{+4.9}_{-2.2}$ s, the half-life of the daughter SF isotope is $0.28^{+0.19}_{-0.08}$ s. The decay chains were observed at the excitation energy of the ^{274}Hs compound nucleus corresponding to the calculated maximum for the ^{226}Ra(^{48}Ca,4n)^{270}Hs reaction (see Table II). Thus, we assigned the six observed decay chains to the ^{270}Hs parent nucleus and obtained a value of 16^{+13}_{-7} pb for the average cross section for the ^{226}Ra(^{48}Ca,4n)^{270}Hs reaction at 41-MeV excitation energy.

In addition to the six observed chains of ^{270}Hs, about three more decays could be detected as ER-SF correlations without registration of an α particle in the focal-plane detector. In the situation when α particles have been detected by the side detector only and thus the beam was not switched off, we could not identify them in the background of random events due to the relatively long half-life of ^{270}Hs.

The ER-SF chains could appear also due to fission of the even-even isotope ^{270}Hs. From calculated partial half-lives of Sg and Hs isotopes and available experimental data on SF probability of even-even isotopes of Rf and Sg, it can not *a priori* be excluded that the $T_{\rm SF}$ value for ^{270}Hs will be comparable with its partial half-life against α decay.

In addition to the 6 SF events shown in Fig. 1, we observed 40 more high-energy signals with $E > 135$ MeV that can be expected for SF of heavy nuclei [1,10–12]; 4 of them were registered by the both focal-plane and side detectors. Thus, from 40%-detection efficiency of both SF fragments,

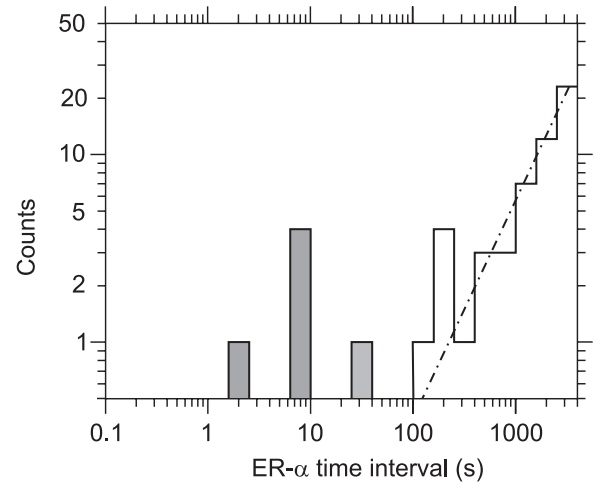

FIG. 2. Time intervals between α particles shown in Fig. 1 and all the preceding ER-like events observed within two ER-α or ER-SF FWHM position resolutions. Part of the histogram referring to the six decay chains shown in Fig. 1 is shaded in gray. Dashed line shows linear fit for random ER-like events.

TABLE II. Experimental and calculated $4n$-evaporation cross sections for the production of ^{270}Hs. Excitation energies E^*_C of the compound nuclei are calculated for Coulomb barrier [15] and masses [22,23]. Cross sections were measured at the excitation energies of the compound nucleus ^{274}Hs of 40 MeV in ^{248}Cm + ^{26}Mg, of 51 MeV in ^{238}U + ^{36}S, and of 37, 41, and 47 MeV in ^{226}Ra + ^{48}Ca reactions.

Reaction	E^*_C (MeV)	σ^{calc}_{4n} (pb) [Ref.]	N events	σ^{exp}_{4n} (pb)	[Ref.]
^{248}Cm + ^{26}Mg	44.5	12 [16]	6	$\approx 3^{+2}_{-1.5}$	[2,3]
^{244}Pu + ^{30}Si	45.6	8 [16]			
^{238}U + ^{36}S	42.0	24 [16]	1	$0.8^{+2.6}_{-0.7}$	[13]
^{226}Ra + ^{48}Ca	32.3	30 [16,17]	0	$\leqslant 3.1$	This
			6	16^{+13}_{-7}	work
			0	$\leqslant 7.1$	

only about 10 of them may be ascribed to SF fragments. From the analysis of time correlations of ER-like and SF-like events [27], the upper limit for the fission branch of ^{270}Hs is set to about 50% and the lower limit for its partial spontaneous fission half-life is 10 s.

At ^{48}Ca energy of $E_{lab} = 234$ MeV, we can set only an upper cross-section limit for the ^{226}Ra(^{48}Ca,3n)^{271}Hs reaction of 11 pb (assuming $T_{1/2} \leqslant 10$ s for ^{271}Hs). On the other hand, at the lower and higher excitation energies of 37 and 47 MeV, the ER-α-SF decay chains of ^{270}Hs were not observed. Here, the upper cross-section limits of the ^{226}Ra(^{48}Ca,4n)^{270}Hs reaction are 3.1 and 7.1 pb, respectively.

For ^{269}Hs, the product of the ^{226}Ra(^{48}Ca,5n) reaction, we refer to its shorter decay branch [28] that should be terminated by spontaneous fission of ^{261}Rf. In terms of decay properties of this isotope (see Ref. [28]), we searched for ER (7.5–16.5 MeV)→α (8.8–9.45 MeV, $\Delta t \leqslant 60$ s)→SF ($\Delta t \leqslant 150$ s) decay chains. Such chains were not found, which results in the upper limit of the cross section for the 5n channel of the ^{226}Ra + ^{48}Ca reaction at $E^* = 47$ MeV of 9.8 pb.

At $E^* = 37$ MeV, we searched for ^{271}Hs by looking for sequences of the type ER (7.5–16.5 MeV)→α (8.7–9.5 MeV, $\Delta t \leqslant 60$ s)→SF ($\Delta t \leqslant 400$ s) within position windows corresponding to two position resolutions. We did not observe chains of the type ER→α→SF$_{off}$ or ER→α→α_{off}→SF$_{off}$ with fission events registered during beam-off time intervals. The upper limit of the cross section for the ^{226}Ra(^{48}Ca,3n)^{271}Hs reaction depends on the unknown half-life of ^{271}Hs. Using ER→α time interval of 8 s for switching the beam off and estimated $T_{1/2}(^{271}\text{Hs}) = 4$ s [3], the upper limit is $\sigma_{3n} \leqslant 8.2$ pb. If the half-life of ^{271}Hs is lower than $T_{1/2}(^{269}\text{Hs})$, the upper cross-section limit for $T_{1/2}(^{271}\text{Hs}) = 1$ s becomes lower; $\sigma_{3n} \leqslant 6.2$ pb. Vice versa, if the half-life of ^{271}Hs is similar or larger than that of ^{269}Hs, the limit increases to 14 pb.

The cross sections for producing ^{270}Hs in the ^{226}Ra + ^{48}Ca experiments, together with the previously known experimental data from other reactions and the calculated cross sections, are combined in Table II.

IV. DISCUSSION

A. Decay properties of ^{270}Hs

For the first time, in this experiment we measured the half-life of the doubly magic nucleus ^{270}Hs ($T_{1/2} = 7.6^{+4.9}_{-2.2}$ s). Its α-particle energy (9.02 ± 0.08 MeV) as well as the half-life of daughter SF isotope ^{266}Sg ($0.28^{+0.19}_{-0.08}$ s) are in agreement with the data determined in ^{248}Cm + ^{26}Mg ($E_\alpha = 8.88 \pm 0.05$ MeV, $T_{SF} = 0.36^{+0.25}_{-0.08}$ s) [3], and ^{238}U + ^{36}S ($E_\alpha = 9.02^{+0.05}_{-0.10}$ MeV, SF decay time 0.023 s) [13] reactions. The measured half-life of even-even ^{270}Hs is in good agreement with the expected probability of allowed α transitions estimated from the measured α-particle energy and using various theoretical T_α versus Q_α relationships (see, e.g., Ref. [29] and references therein). For the partial spontaneous fission half-life of ^{270}Hs, as it was indicated above, only a lower limit was determined ($T_{SF} \geqslant 10$ s).

The decay properties of ^{270}Hs and ^{266}Sg determined in this work, together with the data for other isotopes with $Z = 102$, 104, 106, and 108 [30,31], are presented in Fig. 3. Here are also shown the theoretical expectations following

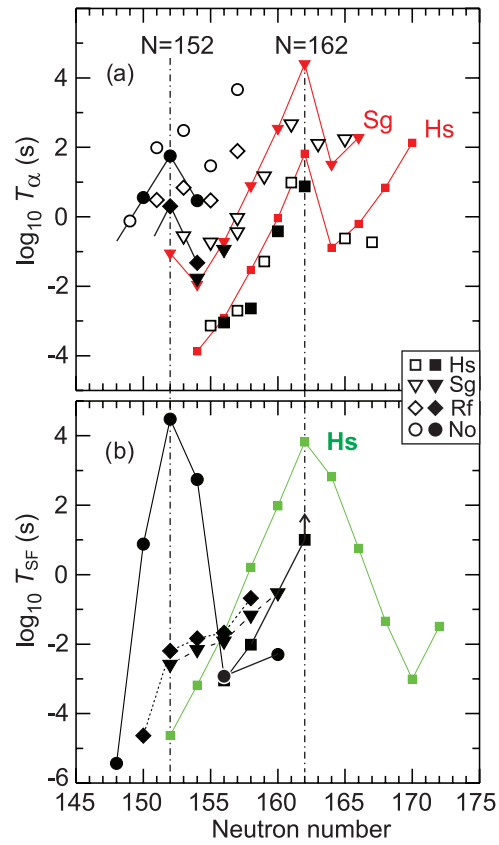

FIG. 3. (Color) Partial half-lives of the nuclei of No, Rf, Sg, and Hs with respect to (a) α decay and (b) spontaneous fission. Solid symbols show even-even isotopes and open ones odd-neutron nuclei. Black lines are drawn to guide the eye; they connect points referring to even-even isotopes. Color lines show calculated half-lives of the even-even isotopes of Sg and Hs (α decay) and Hs (spontaneous fission), calculated in the macroscopic-microscopic nuclear model [32–34].

macroscopic-microscopic calculations [32–34]. As one can see in Fig. 3(a), the considerable decrease of α-decay half-lives observed for Rf, Sg, and Hs in transition from $N = 152$ to 154 substantially changes with increasing neutron number at $Z \geqslant 104$ and $N > 154$. In accordance with the theoretical predictions, by moving off the $N = 152$ shell, a considerable increase of T_α is observed in experiments; this gives evidence of increasing nuclear stability in the ground state upon approaching the next neutron shell at $N = 162$.

Even stronger is the effect of $Z = 108$ and $N = 162$ nuclear shells displayed in the spontaneous fission of these nuclei [Fig. 3(b)]. When going from ^{254}No to ^{256}Rf (both nuclei have $N = 152$, but $\Delta Z = 2$), the probability of spontaneous fission increases by about seven orders of magnitude. This is connected with the change of the fission barrier structure caused by shell effects in deformed nuclei [35]. However, with increasing number of neutrons in the isotopes of Rf and Sg, the spontaneous fission half-life gradually increases. The strongest increase of T_{SF} is observed in Hs nuclei. Of all the even-even isotopes with $Z = 104$–108 shown in Fig. 3(b), the ^{270}Hs ($T_{SF} > 10$ s) isotope is the most stable against spontaneous fission. Note, decrease of proton and neutron numbers in the ^{270}Hs magic nucleus by two, $\Delta Z = \Delta N = 2$ (α decay into ^{266}Sg) increases the probability of spontaneous fission by a factor of more than 30. Such a strong variation of T_{SF} near the peak of stability of Hs isotopes, as well as the experimentally observed trend of growth of $T_{SF}(N)$ when approaching $N = 162$, agree well with model calculations [Fig. 3(b)]. The deviations between absolute values of T_{SF} are explainable taking into account the general difficulties of calculating the probability of spontaneous fission that is a process of tunneling through potential barrier. Generally, the predicted decay properties of the doubly magic nucleus ^{270}Hs are confirmed in the experiment.

B. Cross sections

In the three experiments with three different beam energies, ^{270}Hs was observed only in the excitation energy range $E^* = 38.2$–43.2 MeV, near the calculated maximum of the $4n$-evaporation channel of the ^{226}Ra + ^{48}Ca reaction. The cross section for producing ^{270}Hs in the ^{226}Ra + ^{48}Ca reaction appeared to be about five times higher than in the more asymmetric ^{248}Cm + ^{26}Mg reaction. The excitation energy of the ^{274}Hs compound nucleus at the Coulomb barrier of the ^{226}Ra + ^{48}Ca reaction is $E^*_C = 32$ MeV, lower than that of the case of ^{248}Cm + ^{26}Mg, $E^*_C = 44$ MeV. Despite the fact that the formation of the compound nucleus is more favored in fusion of the more mass-asymmetric nuclei, the shift of the threshold of the ^{248}Cm + ^{26}Mg reaction by $\Delta E^* \approx 10$ MeV results in a reduction of the cross section in the excitation energy range $E^* \approx 40$ MeV (near the maximum of σ_{4n}). For this very reason, in the ^{238}U(^{36}S,$4n$)^{270}Hs reaction with $E^*_C = 42$ MeV the production cross section of ^{270}Hs is only 0.8 pb [13].

An increase of E^* by 10 MeV in the ^{248}Cm + ^{26}Mg reaction would result in an even stronger decrease of the cross section of the $3n$-evaporation channel. Our data differ from those obtained in Refs. [2,3]. Against expectations, in the whole energy range $E^* = 34$–42 MeV in which the production of the isotopes ^{271}Hs and ^{270}Hs in the ^{248}Cm + ^{26}Mg reaction was observed with comparable cross section, we did not detect a single decay event of the isotope ^{271}Hs. Examining various scenarios of interaction of nuclei in the entrance channel of the reactions did not allow us to clarify the reasons for these disagreements and thus needs further investigation.

Now, with the new data on the cross section of the ^{226}Ra(^{48}Ca,$4n$)^{270}Hs reaction, let us consider in a more general sense the reactions of synthesis of heavy and superheavy nuclei ($Z \geqslant 102$).

We would remind the reader that in cold fusion reactions, the doubly magic nuclei ^{208}Pb or ^{209}Bi are used as targets; and advances to higher nuclear charges and masses means using heavier projectiles ranging from ^{50}Ti to ^{70}Zn. In these reactions, the compound nuclei have low excitation energies ($E^* = 12$–20 MeV); their transition to the ground state is accompanied by emission of a single neutron. Note, the production cross section of the lighter isotope of element 108 with $N = 157$ in the ^{208}Pb(^{58}Fe,n)^{265}Hs reaction is about 66 pb [36], which is significantly larger than cross sections for the hot fusion reactions given in Table II.

However, despite this advantage (high survivability of the compound nucleus), the production cross section drops by more than eight orders of magnitude [Fig. 4(a)] when Z_{CN} increases from 102 to 113. Such an effect, as a result of growth of the Coulomb factor $kZ_1Z_2/(A_1^{1/3} + A_2^{1/3})$ by 44% [Fig. 4(c)], is associated with the potential energy surface of the colliding system which causes the hindrance of the formation of compound nuclei with stronger Coulomb interaction.

On the contrary, in hot fusion reactions the magic projectile ^{48}Ca is kept invariable and the atomic number of the compound nucleus is increased by using heavier target nuclei. As opposed to cold fusion, in the more asymmetric reactions of ^{48}Ca with actinide nuclei, the Coulomb repulsion is less but the excitation energy of the compound nucleus is larger. Major losses of evaporation residues occur in the course of cooling down of the heated nucleus by evaporation of multiple neutrons. The total cross section of formation of the isotopes of the given element depends on the thermodynamic properties of the heated compound nucleus and can be generally expressed by a well-known formula

$$\Sigma\sigma_{xn}(E^*, J) = \sigma_{cap} P_{CN}(E^*, J) P_{surv}(B_f, B_n),$$

where σ_{cap} is a capture cross section, $P_{CN}(E^*, J)$ is the probability of the formation of the compound nucleus Z_{CN}, A_{CN} with excitation energy E^* and angular momentum J, and $P_{surv}(B_f, B_n) \sim \prod_{i=1}^{x} \exp[(B_f^i - B_n^i)/T_i]$ is the survivability of the compound nucleus which depends on the fission barrier heights B_f^i and binding energies of neutrons B_n^i of the series of heated nuclei with temperature T_i that are formed in the course of neutron evaporation.

Let us consider first SHE produced in the fusion reactions of the deformed target nuclei, isotopes of U–Cf with ^{48}Ca projectiles that lead to compound nuclei with $Z_{CN} = 112$–118 and $A_{CN} = 286$–297. The Coulomb factor is changed by no more than 6.5%. The excitation energy of the compound nuclei at the Coulomb barrier varies within $E^*_C = 27$–33 MeV (calculated with the Bass barrier [15] without taking into account the effect of orientation of the deformed target nuclei,

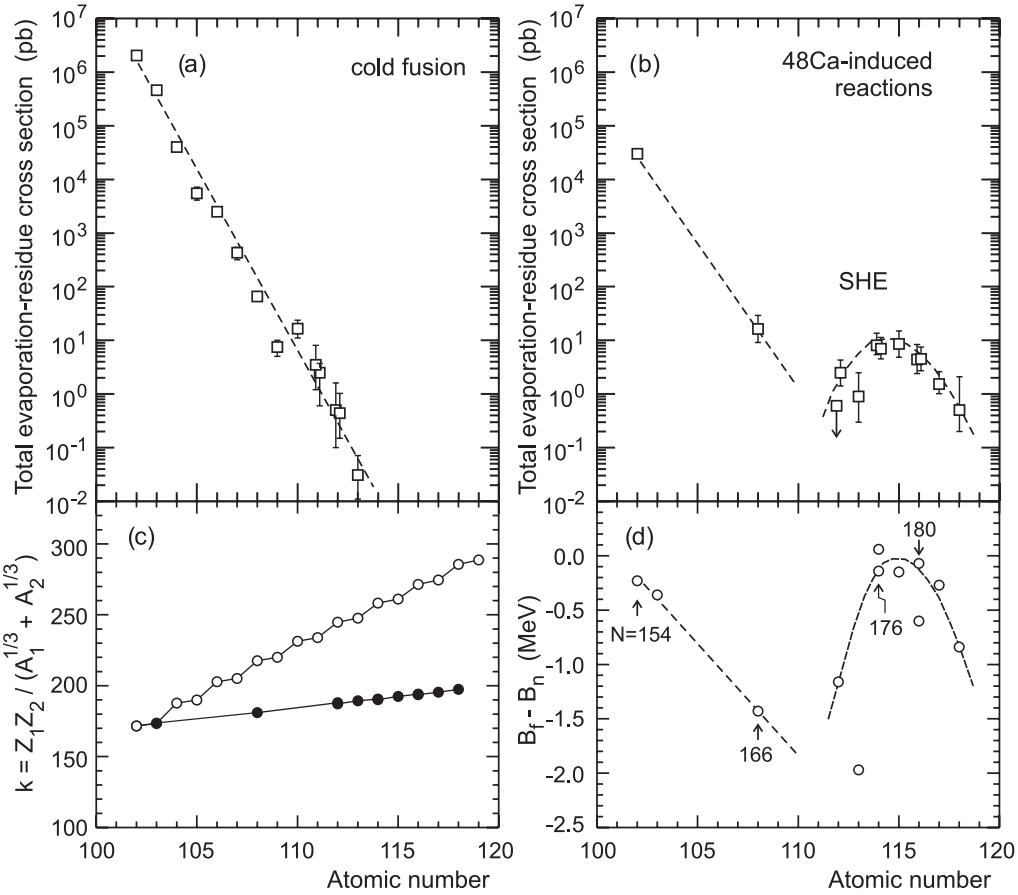

FIG. 4. Maximum cross sections of the production of the isotopes of the heavy elements in (a) cold fusion reactions: ^{208}Pb,^{209}Bi + ^{48}Ca, ^{50}Ti, ^{54}Cr,...^{70}Zn ($E^* = 12$–20 MeV) and (b) hot fusion reactions: ^{208}Pb, ^{226}Ra, ^{233,238}U, ^{242,244}Pu, ^{243}Am, ^{245,248}Cm, ^{249}Bk, and ^{249}Cf + ^{48}Ca ($E^* = 35$–40 MeV). In plot (c), Coulomb factors $Z_1Z_2/(A_1^{1/3} + A_2^{1/3})$ for nuclei in the cold (open circle) and ^{48}Ca-induced (closed circle) reactions are shown. (d) Difference of fission barrier heights (involving nonaxial shapes) and neutron binding energies of the compound nuclei in ^{48}Ca-induced reactions calculated in the macroscopic-microscopic nuclear model [33,37,38] and corrected for the odd-even effect are shown. Arrows show number of neutrons in the compound nucleus with the given atomic number.

which is also practically the same for the actinides). The cross section for producing evaporation residues reaches its maximum at excitation energy $E^* = 35$–40 MeV (hot fusion). The main contribution to the total cross section $(\Sigma\sigma_{xn})^{\max}$, as it follows from the experiments, is due to $3n$- and $4n$-evaporation channels of the reaction and their ratio changes with the nucleonic composition of the compound nucleus [1,4–12].

Because the initial states of the compound nuclei $Z_{\rm CN} = 112$–118 are similar, this allows a uniform description of their transition to ground state via emission of neutrons and γ rays. The calculated survivability of the compound nuclei, which depends on the thermodynamic characteristics of the heated nuclei in the course of their cooling down via emission of neutron(s) and on fission barriers, should thus correlate with evaporation residue cross sections as obtained in the experiment.

In Fig. 4(b), the total cross section $(\Sigma\sigma_{xn})^{\max}$ measured in the experiments in all the reactions of fusion of ^{48}Ca with the target nuclei of Pb, Ra (this work) and with actinide targets U–Cf are shown. The calculated values of $(B_f - B_n)$ are shown in Fig. 4(d) for the compound nuclei having production cross sections given in Fig. 4(b). Comparing these, one can see that the relatively high cross sections for production of evaporation residues in hot fusion reactions with ^{48}Ca are connected with high survivability of the heated compound nuclei. This provides direct evidence of the presence of high fission barriers in these superheavy nuclei.

V. CONCLUSION

^{270}Hs was synthesized in the ^{226}Ra + ^{48}Ca reaction at an excitation energy of $E^* = 41$ MeV with a cross section of 16^{+13}_{-7} pb. ^{270}Hs has an α-SF decay chain with $E_\alpha = 9.02 \pm 0.08$ MeV, and the half-life of the daughter SF isotope ^{266}Sg is $0.28^{+0.19}_{-0.08}$ s. For ^{270}Hs, the half-life $T_{1/2} = 7.6^{+4.9}_{-2.2}$ s was determined for the first time and a lower limit for spontaneous fission was determined to be $T_{\rm SF} \geqslant 10$ s.

In the systematics of the decay properties of the even-even isotopes of elements 102, 104, 106, and 108, one can observe a significant increase of stability when approaching ^{270}Hs. The experimentally determined probabilities of α decay and spontaneous fission of ^{270}Hs agree with the concepts of the macroscopic-microscopic models of its structure as a magic nucleus with closed deformed shells $Z = 108$ and $N = 162$

(see, e.g., Ref. [29] and references therein). It is shown once more that the relatively high cross section for production of heavy and superheavy nuclei in fusion reactions with ^{48}Ca is connected with the presence of a high fission barrier that appears due to nuclear shell effects.

ACKNOWLEDGMENTS

We would like to express our gratitude to the personnel of the U400 cyclotron and the associates of the ion-source group for obtaining intense ^{48}Ca beams; V. I. Krashonkin, A. M. Zubareva, G. N. Ivanov, and V. B. Galinskiy for their help in performing the experiment. One of the authors (Yu.O.) is grateful to K. Siwek-Wilczyńska and J. Wilczyński for calculations of the production cross sections of the superheavy nuclei and for interesting discussions. This work was performed with the support of the Russian Ministry of Atomic Energy and of the Russian Foundation for Basic Research Grant No. 11-02-12066. Much of the support for the LLNL authors was provided under DOE Contract No. DEAC52-07NA27344 with Lawrence Livermore National Security, LLC. These studies were performed in the framework of the Russian Federation/US Joint Coordinating Committee for Research on Fundamental Properties of Matter.

[1] Yu. Ts. Oganessian, J. Phys. G: Nucl. Part. Phys. **34**, R165 (2007).

[2] J. Dvorak, W. Brüchle, M. Chelnokov, R. Dressler, Ch. E. Düllmann, K. Eberhardt, V. Gorshkov, E. Jäger, R. Krücken, A. Kuznetsov, Y. Nagame, F. Nebel, Z. Novackova, Z. Qin, M. Schädel, B. Schausten, E. Schimpf, A. Semchenkov, P. Thörle, A. Türler, M. Wegrzecki, B. Wierczinski, A. Yakushev, and A. Yeremin, Phys. Rev. Lett. **97**, 242501 (2006).

[3] J. Dvorak, W. Brüchle, M. Chelnokov, Ch. E. Düllmann, Z. Dvorakova, K. Eberhardt, E. Jäger, R. Krücken, A. Kuznetsov, Y. Nagame, F. Nebel, K. Nishio, R. Perego, Z. Qin, M. Schädel, B. Schausten, E. Schimpf, R. Schuber, A. Semchenkov, P. Thörle, A. Türler, M. Wegrzecki, B. Wierczinski, A. Yakushev, and A. Yeremin, Phys. Rev. Lett. **100**, 132503 (2008).

[4] S. Hofmann *et al.*, Eur. Phys. J. A **32**, 251 (2007).

[5] S. Hofmann *et al.*, Eur. Phys. J. A **48**, 62 (2012).

[6] L. Stavsetra, K. E. Gregorich, J. Dvorak, P. A. Ellison, I. Dragojević, M. A. Garcia, and H. Nitsche, Phys. Rev. Lett. **103**, 132502 (2009).

[7] P. A. Ellison, K. E. Gregorich, J. S. Berryman, D. L. Bleuel, R. M. Clark, I. Dragojević, J. Dvorak, P. Fallon, C. Fineman-Sotomayor, J. M. Gates, O. R. Gothe, I. Y. Lee, W. D. Loveland, J. P. McLaughlin, S. Paschalis, M. Petri, J. Qian, L. Stavsetra, M. Wiedeking, and H. Nitsche, Phys. Rev. Lett. **105**, 182701 (2010).

[8] Ch. E. Düllmann, M. Schädel, A. Yakushev, A. Türler, K. Eberhardt, J. V. Kratz, D. Ackermann, L.-L. Andersson, M. Block, W. Brüchle, J. Dvorak, H. G. Essel, P. A. Ellison, J. Even, J. M. Gates, A. Gorshkov, R. Graeger, K. E. Gregorich, W. Hartmann, R.-D. Herzberg, F. P. Heßberger, D. Hild, A. Hübner, E. Jäger, J. Khuyagbaatar, B. Kindler, J. Krier, N. Kurz, S. Lahiri, D. Liebe, B. Lommel, M. Maiti, H. Nitsche, J.P. Omtvedt, E. Parr, D. Rudolph, J. Runke, B. Schausten, E. Schimpf, A. Semchenkov, J. Steiner, P. Thörle-Pospiech, J. Uusitalo, M. Wegrzecki, and N. Wiehl, Phys. Rev. Lett. **104**, 252701 (2010).

[9] J. M. Gates, Ch. E. Düllmann, M. Schädel, A. Yakushev, A. Türler, K. Eberhardt, J. V. Kratz, D. Ackermann, L.-L. Andersson, M. Block, W. Brüchle, J. Dvorak, H. G. Essel, P. A. Ellison, J. Even, U. Forsberg, J. Gellanki, A. Gorshkov, R. Graeger, K. E. Gregorich, W. Hartmann, R.-D. Herzberg, F. P. Heßberger, D. Hild, A. Hübner, E. Jäger, J. Khuyagbaatar, B. Kindler, J. Krier, N. Kurz, S. Lahiri, D. Liebe, B. Lommel, M. Maiti, H. Nitsche, J. P. Omtvedt, E. Parr, D. Rudolph, J. Runke, H. Schaffner, B. Schausten, E. Schimpf, A. Semchenkov, J. Steiner, P. Thörle-Pospiech, J. Uusitalo, M. Wegrzecki, and N. Wiehl, Phys. Rev. C **83**, 054618 (2011).

[10] Y. T. Oganessian, F. Sh. Abdullin, P. D. Bailey, D. E. Benker, M. E. Bennett, S. N. Dmitriev, J. G. Ezold, J. H. Hamilton, R. A. Henderson, M. G. Itkis, Yu. V. Lobanov, A. N. Mezentsev, K. J. Moody, S. L. Nelson, A. N. Polyakov, C. E. Porter, A. V. Ramayya, F. D. Riley, J. B. Roberto, M. A. Ryabinin, K. P. Rykaczewski, R. N. Sagaidak, D. A. Shaughnessy, I. V. Shirokovsky, M. A. Stoyer, V. G. Subbotin, R. Sudowe, A. M. Sukhov, Yu. S. Tsyganov, V. K. Utyonkov, A. A. Voinov, G. K. Vostokin, and P. A. Wilk, Phys. Rev. Lett. **104**, 142502 (2010).

[11] Yu. Ts. Oganessian, F. Sh. Abdullin, P. D. Bailey, D. E. Benker, M. E. Bennett, S. N. Dmitriev, J. G. Ezold, J. H. Hamilton, R. A. Henderson, M. G. Itkis, Yu. V. Lobanov, A. N. Mezentsev, K. J. Moody, S. L. Nelson, A. N. Polyakov, C. E. Porter, A. V. Ramayya, F. D. Riley, J. B. Roberto, M. A. Ryabinin, K. P. Rykaczewski, R. N. Sagaidak, D. A. Shaughnessy, I. V. Shirokovsky, M. A. Stoyer, V. G. Subbotin, R. Sudowe, A. M. Sukhov, R. Taylor, Yu. S. Tsyganov, V. K. Utyonkov, A. A. Voinov, G. K. Vostokin, and P. A. Wilk, Phys. Rev. C **83**, 054315 (2011).

[12] Yu. Ts. Oganessian, F. Sh. Abdullin, S. N. Dmitriev, J. M. Gostic, J. H. Hamilton, R. A. Henderson, M. G. Itkis, K. J. Moody, A. N. Polyakov, A. V. Ramayya, J. B. Roberto, K. P. Rykaczewski, R. N. Sagaidak, D. A. Shaughnessy, I. V. Shirokovsky, M. A. Stoyer, V. G. Subbotin, A. M. Sukhov, Yu. S. Tsyganov, V. K. Utyonkov, A. A. Voinov, and G. K. Vostokin, Phys. Rev. Lett. **108**, 022502 (2012).

[13] R. Graeger, D. Ackermann, M. Chelnokov, V. Chepigin, Ch. E. Düllmann, J. Dvorak, J. Even, A. Gorshkov, F. P. Heßberger, D. Hild, A. Hübner, E. Jäger, J. Khuyagbaatar, B. Kindler, J. V. Kratz, J. Krier, A. Kuznetsov, B. Lommel, K. Nishio, H. Nitsche, J. P. Omtvedt, O. Petrushkin, D. Rudolph, J. Runke, F. Samadani, M. Schädel, B. Schausten, A. Türler, A. Yakushev, and Q. Zhi, Phys. Rev. C **81**, 061601(R) (2010).

[14] Yu. Ts. Oganessian, S. N. Dmitriev, A. V. Yeremin, N. V. Aksenov, G. A. Bozhikov, V. I. Chepigin, M. L. Chelnokov, V. Ya. Lebedev, O. N. Malyshev, O. V. Petrushkin, S. V. Shishkin, A. I. Svirikhin, E. E. Tereshatov, and G. K. Vostokin, Phys. Rev. C **79**, 024608 (2009).

[15] R. Bass, in *Proceedings of the Symposium on Deep Inelastic and Fusion Reactions with Heavy Ions, West Berlin, 1979*, edited by W. von Oertzen, Lecture Notes in Physics (Springer, Berlin, 1980), Vol. 117, p. 281.

[16] Z. H. Liu and Jing-Dong Bao, Phys. Rev. C **74**, 057602 (2006).
[17] V. Zagrebaev and W. Greiner, Phys. Rev. C **78**, 034610 (2008).
[18] Yu. Ts. Oganessian, V. K. Utyonkov, Yu. V. Lobanov, F. Sh. Abdullin, A. N. Polyakov, I. V. Shirokovsky, Yu. S. Tsyganov, A. N. Mezentsev, S. Iliev, V. G. Subbotin, A. M. Sukhov, K. Subotic, O. V. Ivanov, A. N. Voinov, V. I. Zagrebaev, K. J. Moody, J. F. Wild, N. J. Stoyer, M. A. Stoyer, and R. W. Lougheed, Phys. Rev. C **64**, 054606 (2001).
[19] A. V. Belozerov *et al.*, Eur. Phys. J. A **16**, 447 (2003).
[20] Yu. Ts. Oganessian *et al.*, *in Proceedings of the 4th International Conference on Dynamical Aspects of Nuclear Fission, Častá-Papiernička, Slovak Republic, 1998* (World Scientific, Singapore, 2000), p. 334.
[21] K. Subotic *et al.*, Nucl. Instrum. Methods Phys. Res., Sect. A **481**, 71 (2002).
[22] G. Audi, A. H. Wapstra, and C. Thibault, Nucl. Phys. A **729**, 337 (2003).
[23] W. D. Myers and W. J. Swiatecki, Nucl. Phys. A **601**, 141 (1996).
[24] F. Hubert, R. Bimbot, and H. Gauvin, At. Data Nucl. Data Tables **46**, 1 (1990).
[25] L. C. Northcliffe and R. F. Schilling, Nucl. Data Tables A **7**, 233 (1970).
[26] K.-H. Schmidt *et al.*, Z. Phys. A: At. Nucl. **316**, 19 (1984).
[27] V. B. Zlokazov, Nucl. Instrum. Methods **151**, 303 (1978).
[28] Ch. E. Düllmann and A. Türler, Phys. Rev. C **77**, 064320 (2008); **78**, 029901(E) (2008).
[29] A. Sobiczewski and K. Pomorski, Prog. Part. Nucl. Phys. **58**, 292 (2007).
[30] Evaluated Nuclear Structure Data File (ENSDF), Experimental Unevaluated Nuclear Data List (XUNDL); http://www.nndc.bnl.gov/ensdf
[31] *Table of Isotopes*, 8th ed., edited by R. B. Firestone and V. S. Shirley (Wiley, New York, 1996).
[32] I. Muntian, S. Hofmann, Z. Patyk, and A. Sobiczewski, Acta Phys. Pol. B **34**, 2073 (2003).
[33] A. Parkhomenko and A. Sobiczewski, Acta Phys. Pol. B **36**, 3095 (2005).
[34] R. Smolańczuk, J. Skalski, and A. Sobiczewski, Phys. Rev. C **52**, 1871 (1995).
[35] Yu. Ts. Oganessian *et al.*, Nucl. Phys. A **239**, 157 (1975).
[36] S. Hofmann *et al.*, Z. Phys. A: Hadrons Nucl. **358**, 377 (1997).
[37] I. Muntian, Z. Patyk, and A. Sobiczewski, Phys. At. Nucl. **66**, 1015 (2003).
[38] M. Kowal, P. Jachimowicz, and A. Sobiczewski, Phys. Rev. C **82**, 014303 (2010) and private communication.